

# On the Steel Fiber Efficiency of UHPC Beams subjected to pure Torsion

Mohammed Ismail<sup>a,b,\*</sup>, Ekkehard Fehling<sup>b</sup>

<sup>a</sup>*University College of Applied Sciences(UCAS), Gaza, Palestine*

<sup>b</sup>*Institute of Structural Engineering (IKI), Kassel University, Kurt-Wolters-Straße 3, D-34125 Kassel, Germany*

## Abstract:

In order to determine the torsional carrying capacity of UHPC beams reinforced with traditional (i.e. longitudinal and transverse) reinforcement in addition to steel fibers, it is essentially important to determine the steel fiber efficiency (i.e. the post cracking tensile strength) in the test beams at the cracking surface at which the failure occurs. Experimental tests on small notched UHPC prisms cast simultaneously with the test beams for torsion in order to determine the steel fiber efficiency showed that the values obtained from these tests may not necessarily reflect the actual fiber efficiency of the torsion test beams at the cracking surface. Experimental tests on notched prisms cut from the torsion test beams at the cracking surface after conducting the torsion tests showed values of fiber efficiency that range between 50 % to 65 % of the values obtained from the first series of tests. The values obtained from the second series of tests were used in an analytical and finite element models to determine the torsional carrying capacity. The comparison between the model predictions and the experimental test results showed very good agreement.

**Keywords:** Finite Element Modeling; Analytical Modeling; UHPC; Steel Fibers; Torsion

## 1. Introduction

Without addition of fibers, Ultra High Performance Concrete (UHPC) is known as a brittle material both in tension and compression. This brittle behavior of this material is not preferable in most cases, such that steel fibers are usually added to the mix to introduce ductility, which results in a product which may be called as Ultra High Performance Fiber Reinforced Concrete (UHPFRC).

Unlike that of the traditional bar reinforcement which has a specific cross sectional area and can be quantified accurately in every cross section along the structural member, the steel fibers are added as volumetric fraction to the UHPC mix and, till now, there is no possible mean to ensure that they have a fully uniform distribution within the mix. Two issues are related to this matter, the first is that the steel fibers may be congested in specific part of the structural member, the other one is the possibility that the steel fibers may accumulate into bundles within the mix. Apart from that is the fact that the contribution of the steel fibers to the bearing capacity is not only related to their distribution along the member, but also to their orientation within the mix [1] and [2]. These uncertainties makes the design for UHPFRC structural elements more difficult, such that detailed investigation of this issue is needed.

## 2. Background

Tests to determine the tensile strength of UHPC without fibers showed an axial tensile strength between 1 ksi (7 MPa) and 1.5 ksi (10 MPa). The failure of UHPC without fibers in axial tension is very brittle, and so no falling branch can be recognized. The UHPFRC shows according to the fibers content, the fibers geometry and the fiber orientation a higher tensile strength and a ductile

post cracking behavior. Figure 1 shows the possible scattering of the falling branch in an axial tensile test. The location of the falling branch in this region depends on the aforementioned factors (e.g., the fibers content, the fibers geometry and the fiber orientation).

After cracking, the tensile resistance of the fiber UHPC is limited either by the strength of the fibers or by the bond strength between fibers and matrix. A failure of the fibers (fiber rupture) occurs only in very long fibers, while shorter fibers are usually pulled out from the matrix. Figure 2 shows the load-deformation behavior of fiber UHPC member with over- and under critical fiber content loaded under axial tension. Fiber efficiency can be defined as the postcracking tensile strength of the UHPFRC structural member.

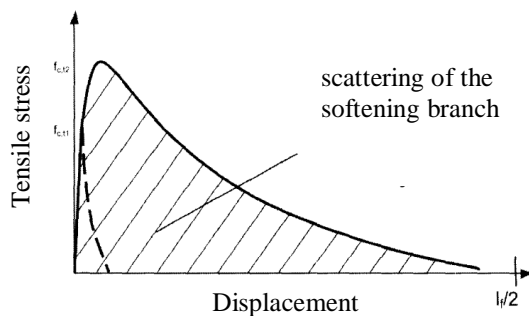


**Figure 1: Scattering of the softening region of UHPFRC under axial tension [3]**

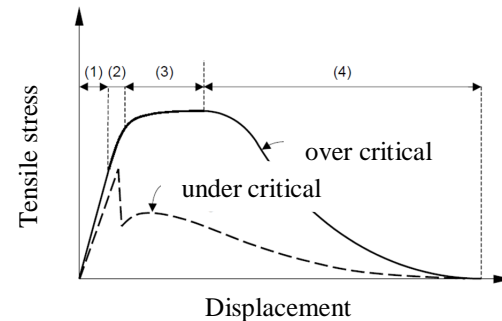


**Figure 2: Stress-crack width diagram of UHPFRC in axial tension [1]**

### 3. Experimental Test Program

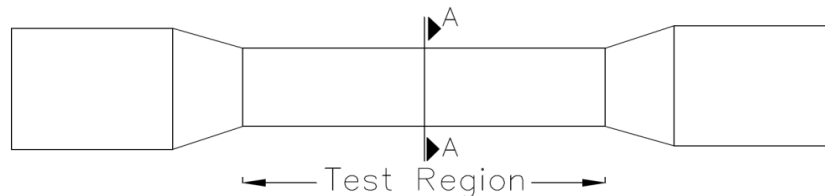
The authors conducted an experimental test program to study the deformation behavior and the torsional carrying capacity of UHPC beams reinforced with different combinations of steel fibers and traditional reinforcement (longitudinal and transverse) [4]. Part of the test program is presented in this paper and is shown in table 1. The beams had square cross section and dimensions of either 7.1 in (180 mm) x 7.1 in (180 mm) x 95 in (2400 mm) or (11 in (280 mm) x 11 in (280 mm) x 59 in (1500 mm) as shown in figure 3.

#### 3.1 Materials

A fine-grained UHPC mix (M3Q) was used. This mix is considered as a further development of the (M2Q) UHPC mix. A detailed description of the input materials of the (M2Q) mix and notes on the production and handling can be found in the research report by Fehling et al. [5]. The average cylinder compressive strength was about 30 ksi (205 MPa) and the average modulus of elasticity was about 6962 ksi (48000 MPa). Steel fibers having tensile strength, length and diameter of about 363 ksi (2500 MPa), 0.7 in (17 mm) and 0.006 in (0.15 mm) were used. Two volumetric ratios of the steel fibers were used within the test program, namely 0.5 % and 0.9 %. Reinforcing steel bars of the type B 500 having a nominal modulus of elasticity of 29000 ksi (200 GPa) were used. According to tests carried out, the yielding strength of the steel bars of 8, 12 and 16 mm diameters was approximated as 80 (550), 83 (570) and 83 ksi (570 MPa) respectively and the ultimate strength as about 91 ksi (625 MPa). More information regarding the casting, treatment of the test beams, the test setup and instrumentation can be found in [4].

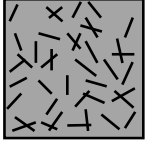
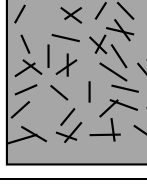
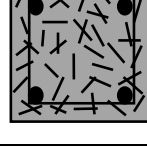
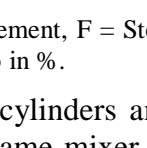
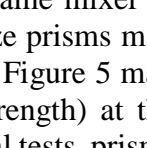
In order to determine the steel fiber efficiency (e.g. postcracking tensile strength), small UHPC notched prisms having dimensions of 1.6 in (40 mm) x 1.6 in (40 mm) x 3.2 in (80 mm)

and notch of about 0.2 in (5 mm) both in width and depth were cast together with the test beams for torsion. Axial tensile tests according to Leutbecher (96) were then carried out. The results of these tests are shown in Figure 5, where the fiber efficiency (postcracking tensile strength) amounts to 0.8 ksi (5.5 MPa) and 1.3 ksi (9 MPa) for steel fiber content of 0.5 % and 0.9 % respectively.



**Figure 3: Shape of the test beam**

**Table 1. The experimental test program**

Series	No. of beams	Fiber vol. %	Longitudinal reinforcement $\rho_L$	Transverse reinforcement $\rho_T$	Beam code	Cross section
1	1	0.5	-	-	UPF(0.5)18	
	1	0.9	-	-	UPF(0.9)18	
2	1	0.5	-	-	UPF(0.5)28	
	1	0.9	-	-	UPF(0.9)28	
3	1	0.5	4Ø12 mm, 1.40 %	Ø8 mm@45 mm, 1.96 %	UL(1.4)T(1.96)F(0.5)18	
	1	0.5	4Ø16 mm, 2.48 %	Ø8 mm@45 mm, 1.96 %	UL(2.48)T(1.96)F(0.5)18	
	1	0.5	4Ø16 mm, 2.48 %	Ø8 mm@30 mm, 2.94 %	UL(2.48)T(2.94)F(0.5)18	

**Legend:** U = UHPC, P = Plain concrete, L = Longitudinal reinforcement, T = Transverse reinforcement, F = Steel fiber, 18 = 180 × 180 mm cross section, 28 = 280 × 280 mm cross section and ( ) = Volumetric ratio in %.

Despite the fact that the torsional test beams and the reference test specimens (cylinders and notched prisms) were cast simultaneously from the same UHPC mix and in the same mixer as described earlier, the distribution and orientation of the steel fibers in the small size prisms may not agree with that in the actual test beams, hence the fiber efficiency presented in Figure 5 may not be representative of the actual steel fiber efficiency (postcracking tensile strength) at the cracking surface of the torsional test beam. After conducting the torsion experimental tests, prisms were cut out from these beams at the location of the cracks and axial tensile tests were carried out. The results of these tests are shown in figure 6. It is obvious that the values of the steel fiber efficiencies for the steel fiber volumes 0.5 % and 0.9 % in Figure 5 and Figure 6 differ considerably. The values of the fiber efficiencies in the second test series amount to 0.52 ksi (3.6 MPa) and 0.67 ksi (4.6 MPa) for fiber content of 0.5 % and 0.9 % respectively. These values will be considered as the actual values of the fiber efficiencies in the following analysis.

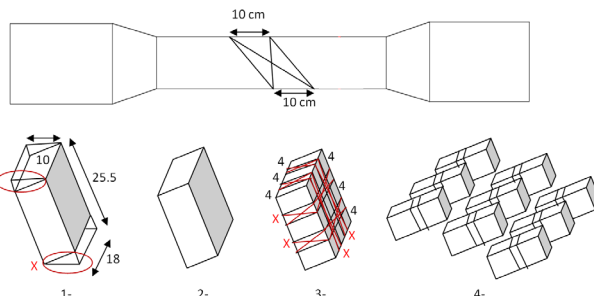


**Figure 4: Notched prisms cut from the test beams after testing under torsion (dimensions in cms)**

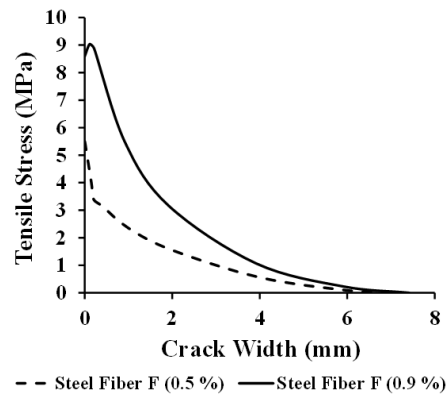


**Figure 5: Average stress-crack width diagram for prisms cast with the test beams**

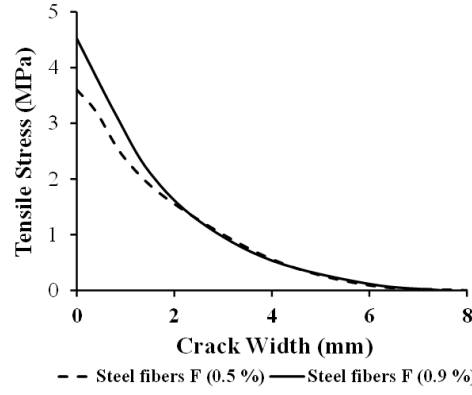


**Figure 6: Average stress-crack width diagram for prisms cut from the test beams**

### 3.2 Test results

Figures 7 and 8 show the torsion test results of the test beams reinforced with steel fibers only and steel fibers in addition to traditional torsional reinforcement respectively. The results of the UHPC beams with steel fibers only show a ductile post cracking behavior with a marginal increase in the ultimate torsional capacity except the beam UPF1(0.9)28 which shows enhanced ultimate capacity. Very high enhancement both in the ductility and torsional capacity are shown in the test results of the beams with both steel fibers and traditional bar reinforcement.

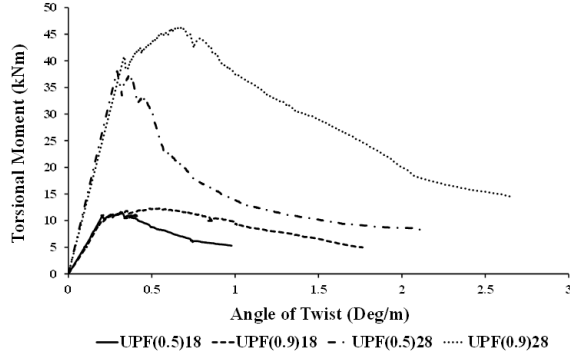


**Figure 7: Torsion test results for UHPC beams with steel fibers only**

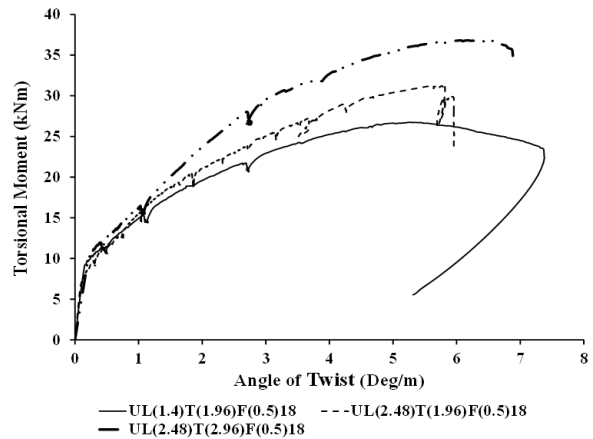


**Figure 8: Torsion test results for UHPC beams with steel fibers and rebars**

#### 4. Analytical Modeling

Based on the well-known thin walled tube theory and space truss analogy for torsion, the author proposed the model presented in [4]. According to own test observations on UHPFRC members under pure torsional load, it was found that at the onset of cracking, the shear cracks develop perpendicular to the principal tensile stress direction. Afterwards, the cracks generally do not only open perpendicular but also slip parallel to their direction as can be seen in figure 9, which is a photo taken for one of the test beams during the conduction of the test. This phenomenon was also confirmed in [5]. In the proposed analytical model, the contribution of the steel fibers along the cracking surface was considered not only in normal direction to the crack but also in tangential direction, such that the steel fibers contributes to the torsional capacity both through tensile and shear forces. The nominal torsional capacity  $T_n$  of fiber-reinforced UHPC member under torsion can be expressed as

$$T_n = \frac{\sigma_{cfo} \times A_w}{\cos \theta \times (h - t_{eff})} \times 2A_k \quad (1)$$

Where  $A_k = X_o \times Y_o = (b - t_{eff}) \times (h - t_{eff})$ ,  $X_o = b - t_{eff}$  and  $Y_o = h - t_{eff}$  as shown in figures 10 and 11. Figure 11 shows that both the tensile and shearing forces are acting on an inclined cross sectional area of  $A_w = t_{eff} \times \frac{h - t_{eff}}{\sin \theta}$ . The tensile force ( $F_{ft}$ ) corresponding to the fiber efficiency ( $\sigma_{cfo}$ ) can be calculated as  $F_{ft} = \sigma_{cfo} \times A_w$ .

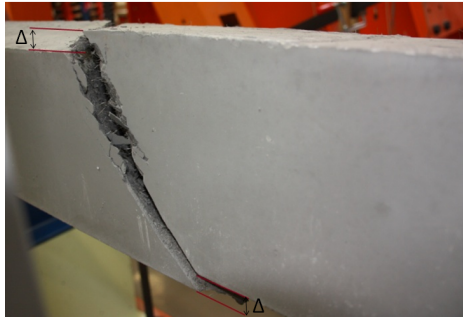


**Figure 9: Deformation parallel to the crack direction**

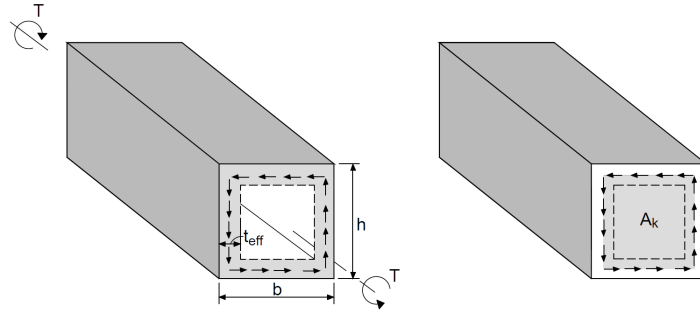


**Figure 10: Thin walled tube (left) and area enclosed by shear flow path (right)**

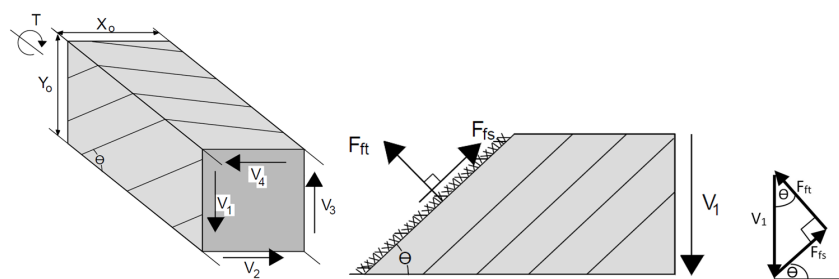


**Figure 11: Shear forces induced in the walls due to torsion (left), Resolution of the shear force  $V_1$  into tensile and shear forces and force equilibrium triangle**

The Eurocode EC 1992 [7] as well as the CEB-FIP model code 90 [8] define the "thin-walled tube" wall thickness for reinforced concrete beams as not less than twice the distance between the

external face and the line joining the axes of the longitudinal reinforcement. As a first approximation, the two codes allow  $t_{eff}$  to be calculated as:

$$t_{eff} = \frac{A_{cp}}{P_{cp}} \quad (2)$$

For the calculation of the cracking torsion  $T_{cr}$ , the ACI Building Code (ACI 318-08) [9] defines the effective wall thickness of the tube as:

$$t_{eff} = \frac{0.75 \times A_{cp}}{P_{cp}} \quad (3)$$

Where  $A_{cp}$  and  $P_{cp}$  are the total area and perimeter of the cross section. A comparison between the estimations of the ultimate torsion of the steel fiber UHPC beams using Equations (2) and (3) and the test results is shown in Table 2.

**Table 2: Comparison between the model and the test results (steel fibers only)**

Beam	$\sigma_{cf0}$ (MPa)	Inclination of cracks $\theta$ (deg)	$T_{ut}$ (test) (kNm)	$T_{n1}$ (Eq2) (kNm)	$T_{n2}$ (Eq3) (kNm)	$T_{n1}/T_{ut}$	$T_{n2}/T_{ut}$
UPF1(0.5)	3.60	47	11.36	11.84	10.42	1.04	0.92
UPF1(0.9)	4.60	47	12.24	15.13	13.32	1.24	1.09
UPF1(0.5)28	3.60	52	38.00	45.80	40.32	1.21	1.06
UPF1(0.9)28	4.60	47	46.32	55.64	48.97	1.20	1.06

For the last three beams in the test program, which are reinforced with steel fibers and traditional (i.e. longitudinal and transverse reinforcement), the nominal torsional capacity is composed of two parts, the first is the contribution of the steel fibers ( $T_f$ ) as calculated in equation 1 using the ACI code formula for  $t_{eff}$ , and the second is the contribution of the space truss model ( $T_t$ ) as found in the Eurocode 2. Table 3 shows very good agreement between the model and test results.

$$T_n = T_f + T_t \quad (4)$$

**Table 3: Comparison between the model and the test results  
(steel fiber, longitudinal and transverse reinforcement)**

Beam	Inclination of cracks $\theta$ (deg)	$T_f$ (kNm)	$T_t$ (EC2) (kNm)	$T_n$ (model) (kNm)	$T_{ut}$ (test) (kNm)	$T_n/T_{ut}$
UL(1.4)T(1.96)F1(0.5)	46	10.42	15.73	26.15	26.72	0.98
UL(2.48)T(1.96)F1(0.5)	41	10.42	19.43	29.85	31.20	0.96
UL(2.48)T(2.94)F1(0.5)	47	10.42	24.85	35.27	32.00	1.10

## 5. Finite Element Modeling

A finite element package called "ATENA" [10] which implements a nonlinear finite element analysis of reinforced concrete structures, was used (ATENA). ATENA can predict the behavior of the structural member not only at ultimate but also throughout the complete load history.

Unlike the normal and high strength concretes, which have well defined material models in ATENA, no standard material model for UHPC with steel fiber is implemented. However, the user

is allowed to define his own material model laws using the general "CC3DNonLinCementitious2user" material model. These laws are:

- Tensile and post cracking softening behavior
- Compression behavior
- Effect of lateral compression on tensile strength
- Effect of lateral tensile strain on the compression capacity
- Post cracking shear strength
- Post cracking shear stiffness
- Other input parameters, like:
  - Tensile and compressive strength
  - Modulus of elasticity and Poisson's ratio

Details about the material laws used for UHPC with steel fibers in ATENA, the boundary conditions and the finite element mesh can be found in (Ismail 196). What is important to note that the tensile stress – crack width diagrams produced by prisms cut from the test beams and presented in figure 6 have been used in this analyses and very good agreement can be achieved between the test results and the model predictions as shown in figure 12.

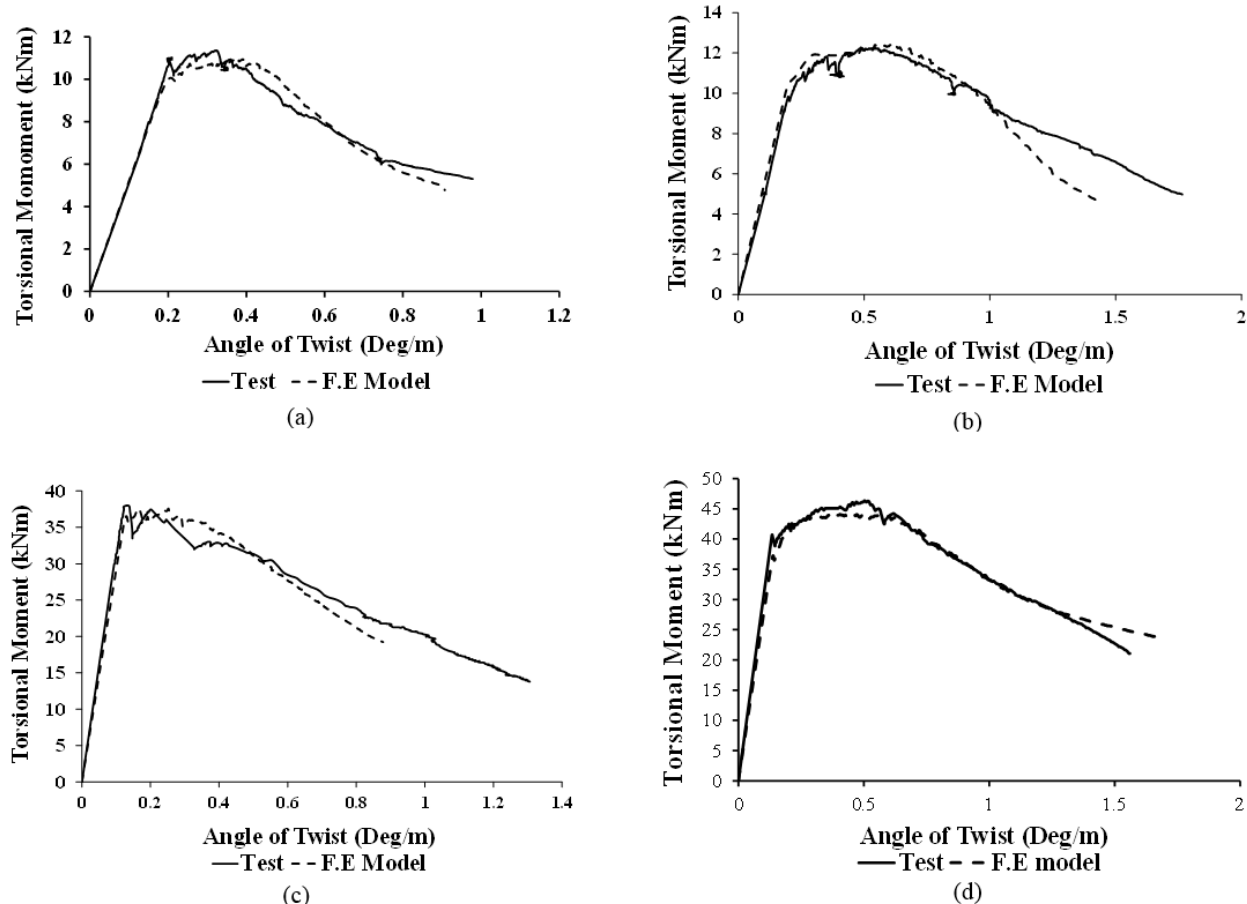


**Figure 12: Comparison between test results and F.E prediction for the test beams:  
 a) UPF(0.5)18, b) UPF(0.9)18, c) UPF(0.5)28 and d) UPF(0.9)28**

## 6. Discussion and Conclusions

Within the framework of a test program conducted at the university of Kassel to investigate the torsional carrying capacity and the deformation behavior of UHPC beams reinforced with steel fibers and bar reinforcement, the issue related to the fiber efficiency (i.e. the post cracking tensile strength) of UHPFRC in the sense of the way used to determine its value has been investigated.

Axial tensile tests on notched prisms have been conducted on two types of specimens, the first type consists of prisms cast simultaneously and from the same UHPFRC mix used for the torsional test beams. The second type was for prisms cut from the torsional test beams at the locations of the cracks that caused failure of the beam under pure torsional loading. Results of the axial tensile test show that the second type of specimens yield reduced values of the fiber efficiency, where the fiber efficiencies of these specimens with steel fibers content of 0.5 % and 0.9 % amounts only to 65 % and 50 % respectively from the results of the first test prisms. This can be attributed to the different distribution and orientation of the steel fibers in the torsional test beams than that in the prisms cast simultaneously.

In order to confirm this experimental conclusion, the test results (i.e. values of fiber efficiencies) obtained from the second series of prisms have been used to predict the torsional carrying capacity once using an analytical model and once using a F. E. Model. Very good agreement between the predictions of both models and the torsional test results have been obtained which in turn confirms our conclusion.

## 7. References

- [1] Leutbecher, T., "Rissbildung und Zugtragverhalten von mit Fasern und Stabstahl bewehrtem Ultrahochfesten Beton (UHPC)," *Structural Materials and Engineering Series*, No. 9, Kassel University Press GmbH, ISBN: 978-3-89958-374-8. 2008.
- [2] Stürwald, S., "Rissentwicklung bei kombiniert bewehrten UHPC-Balken," 53. *Forschungskolloquium der Deutschen Ausschusses für Stahlbeton*. Kassel, Germany. ISBN: 978-3-86219-395-0. 9-10, October, 2012.
- [3] Schmidt, M. et al., "Sachstandsbericht Ultrahochfester Beton", Deutscher Ausschuss für Stahlbeton (DAfStb)- Heft 561, Erste Auflage, Beuth Verlag GmbH, Berlin. ISBN: 978-3-410-65045-4. 2008.
- [4] Ismail, M., "Behavior of UHPC structural members subjected to pure torsion", PhD Dissertation. *Structural Materials and Engineering Series*, No. 24. Kassel University Press, ISBN: 978-3-86219-952-5. 2015
- [5] Fehling, E., Schmidt M., Teichmann T. and Bunje K., "Entwicklung, Dauerhaftigkeit und Berechnung Ultra-Hochfester Beton (UHPC)", Forschungsbericht an die DFG, *Structural Materials and Engineering Series*, No. 1. Kassel University Press GmbH, ISBN: 3-89958-108-3, 2005.
- [6] Walraven, J. C., "Aggregate interlock - A Theoretical and Experimental Analysis". *Doctoral Thesis*, Delft University of Technology. Netherland. 1980.
- [7] Eurocode 2: Design of concrete structures - Part 1-1: General rules and rules for buildings (2004-2012). European Committee for Standardization (CEN), Brussels
- [8] CEB-FIP Model-Code 1991. Design Code. Comite Euro-International du Beton: Bulletin d'information No. 213/214, Lausanne, Switzerland.

- [9] ACI 318-08: "Building Code Requirements for structural concrete (ACI 318-08) and commentary (ACI 318R-08)". 1st Printing 2008. American Concrete Institute, Michigan, USA: Farmington Hills.
- [10] ATENA Program Documentation, Cervenka Consulting, Prague, Czech Republic. 2013.